Veterinary Microbiology 236 (2019) 108395

Contents lists available at ScienceDirect

Veterinary Microbiology

journal homepage: www.elsevier.com/locate/vetmic

Identification of three site mutations in nonstructural protein 1β, glycoprotein 3 and glycoprotein 5 that correlate with increased interferon α resistance of porcine reproductive and respiratory syndrome virus

Jia Su, Xinhui Zhang, Bicheng He, Xinna Ge, Jun Han, Lei Zhou*, Xin Guo*, Hanchun Yang

Key Laboratory of Animal Epidemiology of the Ministry of Agriculture, College of Veterinary Medicine, China Agricultural University, Beijing 100193, People's Republic of China

ARTICLE INFO

Keywords:
Porcine reproductive and respiratory syndrome virus (PRRSV)
Evolution
Mutation
Interferon α
JAK-STAT pathway
Phosphorylation

ABSTRACT

Porcine reproductive and respiratory syndrome virus (PRRSV) is an economically significant pathogen that has been recognized for its genetic variation, rapid evolution, and immune suppression. Type I interferons (IFNs) play an important role in host defense against viral infection by inducing many antiviral effectors, which might be a selective pressure driving viral evolution towards IFN resistance. To investigate the IFN resistance-related variation of PRRSV genome under IFN selective pressure and explore the molecular mechanism of IFN sensitivity changes, PRRSV strain JXwn06 was serially propagated in porcine pulmonary alveolar macrophages (PAMs) with IFNα treatment for 45 passages and 3 rounds of purification. Four mutant strains named JX-αP51n (n = 1, 2, 3 and 4) with reduced IFNα sensitivity were selected; the strains showed a 100-fold higher titer than the passaging-control strain JX-P51 in IFNα-treated PAMs. IFNα-resistant strains were found to antagonize the IFNα-activated JAK-STAT signaling pathway to a greater extent than the nonresistant strain by down-regulating the expression level of IFNα-activated pJAK1 through interfering with phosphatase. Furthermore, the PRRSV genetic variations interacting with IFNα were identified by full genomic sequencing and alignment. Among these mutations, amino acid substitutions in nsp1β (E87 G), GP3 (F143 L) and GP5 (Y136 H) were found to correlate with increased IFNα resistance by enhancing the suppression effect on pJAK1, which could be further increased if these three substitution sites were combined. These findings provide some novel evidence for understanding PRRSV genetic variation under host selective pressure and viral evolution strategies to evade the host innate immune response.

1. Introduction

Porcine reproductive and respiratory syndrome (PRRS) is regarded as one of the most economically significant viral diseases worldwide and has greatly impacted the swine industry since it was first reported at the end of the 1980s (Keffaber, 1989). PRRS is characterized by reproductive failure in pregnant sows and respiratory distress in pigs of all ages (Albina, 1997). The etiological agent, porcine reproductive and respiratory syndrome virus (PRRSV), is an enveloped RNA virus, which is classified into the genus *Porartevirus* of the family *Arteriviridae* in the order *Nidovirales* (Kuhn et al., 2016). The PRRSV genome is approximately 15 kb in length, with 12 identified open reading frames (ORFs) (Lunney et al., 2016). ORF1a and ORF1b encode two replicase polyproteins, pp1a and pp1ab, which can be proteolytically processed into at least 16 viral nonstructural proteins (nsps) that are involved in viral replication, transcription, modulation of the host immune system and virulence (Fang et al., 2012). The remaining ORF2a, ORF2b, ORFs3-7 and ORF5a encode structural proteins involved in virus infectivity, neutralizing antibody elicitation, etc. (Snijder et al., 2013).

IFNα/β, two major type I interferons, display diverse biological functions in antiviral and antiproliferative mechanisms (Stetson and Medzhitov, 2006). The secreted IFNs bind their cognate receptors and initiate signaling through the Janus kinase/signal transducer and activator of transcription (JAK-STAT) pathway, resulting in the transcriptional induction of interferon-stimulated genes (ISGs), which encode antiviral effectors (Schoggins et al., 2011).

The outcome of viral infection can be affected by both IFN induction and the IFN sensitivity of a virus. To successfully invade host cells, PRRSV interferes with various host innate immune processes, including affecting IFN production (Buddaert et al., 1998; Calzada-Nova et al.,

* Corresponding authors at: Department of Preventive Veterinary Medicine, College of Veterinary Medicine, China Agricultural University, 2 Yuanmingyuan West Road, Haidian District, Beijing, 100193, People's Republic of China.
E-mail addresses: leosj@cau.edu.cn (L. Zhou), guoxin@cau.edu.cn (X. Guo).

https://doi.org/10.1016/j.vetmic.2019.108395
Received 17 March 2019; Received in revised form 17 August 2019; Accepted 18 August 2019

2011; Han et al., 2017), interfering with the IFN-induced signaling pathway (Chen et al., 2010; Patel et al., 2010; Wang et al., 2013a; b), and disturbing the activities of ISGs (Dong et al., 2018; Patel et al., 2010; Sun et al., 2012). On the other hand, as an RNA virus with low replication fidelity, PRRSV is characterized by its genetic variation and rapid evolution (Han et al., 2017). Replication through an error-prone process may support the evolution of genetic variants resistant to the host antiviral response. It has been previously reported that the immunopressure of continuously propagating PRRSV in MARC-145 cells with pretreatment of IFNβ at relatively low concentrations, could accelerate the genetic variation of PRRSV, especially in ORF5, nsp2 and ORF3 coding regions (He et al., 2013). It was also found that site mutations in nsp1β correlate with inhibition of IFN-induced downstream signaling (Wang et al., 2013a) and that GP5 facilitates viral replication by inhibiting IRF-3 activation (Xiong et al., 2015). Therefore, it will be interesting to investigate the IFN resistance-related variation under IFN selective pressure and explore the molecular mechanisms of the virus that contribute to the change in IFN sensitivity.

In this study, IFNα-resistant PRRSV strains were selected by serial passaging in PAMs treated with exogenous IFNα. The variation analyses and subsequent confirmation by reverse genetics suggested that at least three mutant sites occurring in nsp1β, GP3 and GP5 lead to the reduction of PRRSV interferon sensitivity. Additionally, the mutant sites correlate with the increased capability of the virus to antagonize the IFNα-activated JAK-STAT signaling pathway by reducing the expression level of IFNα-activated pJAK1 through interfering with phosphatase.

2. Materials and methods

2.1. Cells and virus

MARC-145 cells were cultured in Dulbecco's modified Eagle medium (DMEM) (Thermo Fisher Scientific, Waltham, MA, USA) supplemented with 10% fetal bovine sera (FBS) (HyClone Laboratories Inc., South Logan, UT, USA) at 37 °C in a humid 5% CO_2 atmosphere. Porcine pulmonary alveolar macrophages (PAMs) were prepared from 35- to 42-day-old specific pathogen-free (SPF) pigs as previously described (Zhang et al., 2009) and grown in RPMI 1640 medium (Thermo Fisher Scientific, Waltham, MA, USA) supplemented with 10% FBS, 50 U/ml penicillin, 50 mg/ml streptomycin, and maintained in a 37 °C humidified chamber with 5% CO_2. The highly pathogenic PRRSV (HP-PRRSV) strain JXwn06 (GenBank accession No. EF641008.1) (Zhou et al., 2009a,2009b) was identified and preserved by our laboratory.

2.2. Selecting IFNα-resistant strains

PAMs seeded in 24-well plates were pretreated with IFNα at a concentration of 200 U/ml for 12 h and subsequently infected with JXwn06 virus at a multiplicity of infection (MOI) of 0.01. Following incubation at 37 °C for 1 h, the inoculum was replaced with fresh medium containing IFNα ranging from 200 U/ml to 1000 U/ml. The inoculated cells were then maintained at 37 °C with 5% CO_2 for daily observation of the cytopathic effect (CPE) to determine the optimal IFNα concentration for PAM treatment. Then, PRRSV was serially passaged in the PAMs treated with the optimal concentration of IFNα based on the test above, with three independent repeat patches. The titers of the harvested virus were tested every 5 passages by $TCID_{50}$ assay to roughly evaluate the IFNα resistance of the virus. Additionally, the JXwn06 virus passaged in the PAMs without the addition of exogenous IFNα formed the passaging control.

After forty-five serial passages in IFNα-treated PAMs, the harvested virus was purified by limiting-dilution infections on PAMs that were treated with IFNα (200 U/ml) in 96-well plates. The samples from the CPE-positive wells in the highest dilution were collected for the next round of purification. After 3 rounds of purification, the virus was passaged in the IFNα-treated PAMs three further times to increase the viral culture volume.

2.3. IFNα sensitivity evaluation

To measure the IFNα sensitivity of the IFNα-selected virus or mutagenic virus, primary PAMs were pretreated with 200 U/ml IFNα for 12 h. Then, cells were infected with the respective virus at an MOI of 0.01. Cells were washed three times with phosphate-buffered saline (PBS) (1 ×, pH 7.4) after 1 h incubation, and then the fresh media with IFNα at a final concentration of 200 U/ml was added after removing the PBS. The inoculum was collected at 12 h, 24 h, 36 h, 48 h, 60 h and 72 h post-infection (pi) to determine the viral titers by $TCID_{50}$ assay, as previously described (Li et al., 2014). The titer of each virus passaged in the PAMs without IFNα treatment was also tested in parallel to calculate the titer difference relative to virus passaged with IFNα treatment. Three independent repeats were carried out for all tests.

2.4. Genomic analysis of the IFNα-resistant PRRSV strains

Viral RNA was extracted from infected PAMs by using TRIzol reagent (Thermo Fisher Scientific, Waltham, MA, USA), and 14 overlapping fragments covering the whole genome of PRRSV were amplified by reverse transcription-PCR (RT-PCR) as described previously (Zhou et al., 2009a,2009b). The 5′ untranslated region (5′ UTR) and 3′ UTR were amplified by using either the 5′ UTR Full RACE kit or the 3′ UTR Full RACE kit (TaKaRa, Dalian, China) according to the manufacturer's instructions. The PCR products were purified with the EasyPure Quick Gel Extraction kit (Transgen, Beijing, China) and subsequently cloned into the pJET1.2 vector (Thermo Fisher Scientific, Waltham, MA, USA). Then, all viral fragments were submitted for sequencing by BioSune (Beijing, China) using the Sanger sequencing approach and were assembled into full-length consecutive sequences. The genomic sequences of the IFNα-resistant virus and virus in the parallel control group were compared with the reference sequence of JXwn06 by using Megalign (DNASTAR, Madison, AL, USA).

2.5. Recovery of infectious mutant virus

The variation sites in the genome of IFNα-resistant PRRSV strains were mapped (Table 2). In total, six amino acid residue mutations located in nsp1β (position 87), GP3 (position 87 and 143), GP5 (position 37 and 136) and M (position 128), which might be related to the increased IFNα resistance of the virus, were selected for further investigation. The viruses containing the site mutations were constructed and rescued by using the PRRSV reverse genetics system, following the similar strategy described previously, with slight modification (Xu et al., 2018). Briefly, fragment A, containing the nsp1β-coding region, or fragment D, containing GP3-, GP5- and M-coding regions of pWSK-JXwn with the unique flanking restriction enzyme site pairs *SwaI/BstB*I and *AscI/Pac*I, respectively, were amplified by using KOD DNA polymerase (TOYOBO, Japan), with the full-length PRRSV plasmid as the template. Then, the purified PCR products were cloned into pJET1.2/blunt to construct the intermediate plasmids pJET1.2-A or pJET1.2-D. The target nucleotide substitutions were imported into the plasmid by using a fast mutagenesis kit (TransGen, Beijing, China). Subsequently, the target fragments were assembled into the full-length plasmid pWSK-JXwn by using homologous recombination with the ClonExpress II One Step Cloning kit (Vazyme, Nanjing, China) to generate the full-length infectious cDNA clone with corresponding mutation site(s). All constructed fragments and the mutation sites in the full-length infectious clone plasmid were confirmed by sequencing.

To recover the infectious PRRSV from the constructed infectious clones, MARC-145 cells seeded at approximately 80% confluency in 6-well plates were transfected with 2.5 μg of the full-length plasmid DNA using 7.5 μl of Lipofectamine LTX (Thermo Fisher Scientific, Waltham,

Table 1
Primers used in this study.

Primer[a]	Sequence (5′-3′)[b]	Usage
ISG54-F	CTGGCAAAGAGCCCTAAGGA	Quantification of ISG54 gene transcription level
ISG54-R	CTCAGAGGGTCAATGGAATTCC	
RNase L-F	GCCAGACCTAGTGGCTTCTG	Quantification of RNase L gene transcription level
RNase L-R	AGAGGCCCAGAGAGTTGTGA	
PPIA-F	AAGGTTCCTGCTTTCACAGAATAAT	Quantification of PPIA gene transcription level
PPIA-R	AATTTCTCTCCATAGATGGACTTGC	
nsp1β-87-F	CTGACACTGTCCCTG*G*AGGAAACTGC	Introduction of mutation into nsp1β
nsp1β-87-R	*C*CAGGGACAGTGTCAGCGGGGAGG	
ORF3-87-F	GTAGTGAGAACGATC*G*TGACGAACTA	Introduction of mutation into ORF3
ORF3-87-R	*C*GATCGTTCTCACTACATCGGTCA	
ORF3-143-F	GACATCAAGCACCAAC*T*CATCTGCGC	Introduction of mutation into ORF3
ORF3-143-R	*G*TTGGTGCTTGATGTCAACATAAA	
ORF5-37-F	AGCAACAACAACAGCCCTCATATTCA	Introduction of mutation into ORF5
ORF5-37-R	*G*GCTGTTGTTGTTGCTGGCGTTGA	
ORF5-136-F	TGCATGTCCTGGCGCC*A*CTCTTGTAC	Introduction of mutation into ORF5
ORF5-136-R	*G*GCGCCAGGACATGCAGTTCTTCG	
ORF6-128-F	ATCCGATTGCGGCAA*G*TGATAACCAC	Introduction of mutation into ORF6
ORF6-128-R	*C*TTGCCGCAATCGGATGAAAGCCC	
JX-A(*Swa*I)-Fusion-F	CAGAGCTGGTTTAGTATTTAAATATGACGTATAGGTGTTGGCTCTATG	Fragment amplification and fusion
JX-A(*BstB*I)-Fusion-R	CCTCCCCCTGAAGGCTTCGAAATTTGCCTGATCTTTAGTCCATTCA	
JX-D(*Asc*I)-Fusion-F	CAATGATGCGTTTCGGGCGCGCCAGAAAGGGAAAATTTATAAAGCT	Fragment amplification and fusion
JX-D(*Pac*I)-Fusion-R	GAGGAGGCTGGGACCATGCCGGCCTTAATTAATTTTTTTTTTTTTTTTTTTTTTTTTTTTTTTTTTTTTTTTTTAATTACGGCC	

[a] F denotes forward PCR primer; R denotes reverse PCR primer.
[b] Restriction sites are underlined. Mutated nucleotides are shown as italics.

MA, USA) according to the manufacturer's instructions. At 48 h post-transfection, the recovered viruses were harvested for examination by indirect immunofluorescence assay (IFA) using the PRRSV N-specific monoclonal antibody (mAb) SDOW17 (Rural Technologies, Brookings, SD, USA) as previously described (Meng et al., 1996). The mutation sites in the recovered virus were further confirmed by RT-PCR and sequencing.

2.6. Quantitative reverse transcription-PCR (qRT-PCR)

To evaluate the mRNA transcription level of ISGs in the PAMs infected with IFNα-resistant virus, the relative expression of two representative ISGs, ISG54 and RNase L, which have been reported to be regulated by PRRSV, were analyzed by qRT-PCR, carried out as described previously with the primers listed in Table 1 (He et al., 2018; Patel et al., 2010; Zhao et al., 2017). PAMs were infected with the respective virus with at an MOI of 0.01. At 24 h post-infection, the cells were treated with 200 U/ml of IFNα for 8 h, and then the total RNA was extracted by using TRIzol reagent (Thermo Fisher Scientific, Waltham, MA, USA). The cDNA synthesized by using the HiScript II Q RT SuperMix for qPCR kit (Vazyme, Nanjing, China) was then submitted for qRT-PCR with 2× Power SYBR Green Master Mix (Thermo Fisher Scientific, Waltham, MA, USA). The relative expression of ISG mRNA was quantified with the $2^{-\Delta\Delta Ct}$ method after normalization to the peptidylprolyl isomerase A (PPIA) gene and displayed as the relative fold change compared with the IFNα-untreated PAMs (Dong et al., 2018).

2.7. Western blot analysis

Western blot was performed following the standard protocol established in our laboratory. Briefly, PRRSV-infected or mock-infected PAMs cultured in 6-well plates were lysed with 150 μl/well of radioimmunoprecipitation assay (RIPA) buffer (Beyotime, Shanghai, China) supplemented with the protease inhibitor phenylmethylsulfonyl fluoride (PMSF) (Beyotime, Shanghai, China). Total proteins in the lysate were quantified by a bicinchoninic acid (BCA) protein assay kit (Thermo Fisher Scientific, Waltham, MA, USA). Then, equal amounts of protein lysate from each sample was separated by discontinuous SDS-PAGE under reducing conditions, with stacking and resolving gels containing 5% and 12% acrylamide, respectively, and then proteins were transferred to a polyvinylidene difluoride (PVDF) membrane (Millipore, Bedford, MA, USA) using a semidry apparatus. After blocking with 5% (w/v) skim milk in 1 × PBS, the membranes were incubated first with a primary antibody and then with an appropriate horseradish peroxidase (HRP)-conjugated secondary antibody. The enhanced chemiluminescence (ECL) system (Vigorous, Beijing, China) was utilized to detect the blotted proteins. Protein bands were quantitated using Image Studio (LI-COR, Lincoln, NE, USA) software and normalized to β-actin.

2.8. Antibodies and reagents

Antibodies against JAK1, phosphos-JAK1 (Tyr1022/1023), STAT1, phospho-STAT1 (Tyr701), STAT2 and phosphos-STAT2 (Tyr690) were all purchased from Cell Signaling Technology (Beverly, MA, USA). The mAb against PRRSV N protein was kindly provided by professor Ping Jiang (Nanjing Agriculture University, Nanjing, China). The mouse anti-IFNAR1 and anti-IFNAR2 antibodies (Abcam, Cambridge, UK), anti-β-actin mAb (Sigma-Aldrich, MO, USA) and horseradish peroxidase (HRP)-conjugated goat anti-mouse or goat anti-rabbit IgG (Beyotime, Shanghai, China) were also used in this study. IFNα was purchased from R&D (R&D Systems, MN, USA). Sodium orthovanadate (Na_3VO_4) was purchased from Sigma Aldrich (St. Louis, MO, USA).

2.9. Ethics statement

The animal experiment for primary PAM preparation was approved by the Laboratory Animal Ethical Committee of China Agricultural University, with the approval No. CAU20150601-2.

2.10. Statistical analysis

GraphPad Prism software (version 5.0) was used to determine the

Table 2
Amino acid substitution of JX-P51, JX-αP51-1, JX-αP51-2, JX-αP51-3 and JX-αP51-4.

JXwn06→JX-P51/JX-αP51-1/JX-αP51-2/JX-αP51-3/JX-αP51-4				
	Loci (5′)[a]	nucleotide (amino acid)	Loci (5′)[a]	nucleotide (amino acid)
nsp1α	509	C→C/G/C/C/C (P→P/R/P/P/P)		
nsp1β	41	T→C/T/T/T/T (V→A/V/V/V/V)	173	C→C/T/C/T/C (S→S/F/S/F/S)
	260	A→G/G/G/G/G (E→G/G/G/G/G)[b]	499	A→A/A/A/A/G (S→S/S/S/S/G)
	503	T→C/T/T/T/T (L→P/L/L/L/L)	572	A→A/G/A/A/G (E→E/G/E/E/G)
nsp2	7	A→A/A/A/G/A (K→K/K/K/E/K)	8	A→A/G/A/A/A (K→K/R/K/K/K)
	22	C→C/T/C/T/T (P→P/S/P/S/S)	369	T→T/T/T/A/T (H→H/H/H/Q/H)
	394	A→A/G/A/A/A (M→M/V/M/M/M)	460	T→T/T/T/C/T (S→S/S/S/P/S)
	526	C→C/C/T/C/C (H→H/H/Y/H/H)	539	G→G/G/G/G/A (S→S/S/S/S/N)
	550	G→G/G/G/G/A (A→A/A/A/A/T)	658	G→A/G/G/G/G (D→N/D/D/D/D)
	926	C→T/C/T/C/C (S→L/S/L/S/S)	1111	T→T/T/C/T/T (S→S/S/P/S/S)
	1466	C→C/C/T/C/C (P→P/P/L/P/P)	1525	C→C/C/T/C/C (R→R/R/C/R/R)
	1606	C→C/T/C/C/C (H→H/Y/H/H/H)	1611	G→G/C/G/G/C (Q→Q/H/Q/Q/H)
	1661	T→T/C/T/T/T (F→F/S/F/F/F)	1735	A→A/A/C/A/A (I→I/I/L/I/I)
	1817	A→G/A/G/A/A (K→R/K/R/K/K)	1835	T→T/C/T/T/T (I→I/T/I/I/I)
	1982	T→T/T/T/C/T (M→M/M/M/T/M)	2000	C→A/A/C/C/C (T→K/K/T/T/T)
	2005	G→T/T/G/G/G (A→S/S/A/A/A)	2062	C→T/T/T/T/T (L→F/F/F/F/F)[b]
	2267	C→C/T/C/T/T (P→P/L/P/L/L)	2284	A→A/A/G/A/A (M→M/M/V/M/M)
	2753	T→T/T/T/C/T (L→L/L/L/P/L)	2855	C→C/C/T/C/C (A→A/A/V/A/A)
	2869	C→C/T/C/C/C (H→H/Y/H/H/H)	2905	A→A/A/A/A/G (I→I/I/I/I/V)
nsp3	173	T→T/T/T/G/T (L→L/L/L/W/L)		
nsp4	62	G→A/G/G/G/G (G→D/G/G/G/G)	532	A→G/A/A/A/A (I→V/I/I/I/I)
nsp5	74	C→C/C/C/T/C (P→P/P/P/L/P)	502	T→G/T/T/T/T (F→V/F/F/F/F)
nsp7α	320	A→T/A/A/A/A (H→L/H/H/H/H)	400	C→C/C/C/T/C (P→P/P/P/S/P)
nsp7β	56	G→G/A/G/G/G (R→R/K/R/R/R)	107	T→T/T/G/T/T (F→F/F/C/F/F)
	244	G→G/A/G/A/A (D→D/N/D/N/N)	323	A→A/A/G/A/A (Q→Q/Q/R/Q/Q)
nsp9	133	A→A/A/A/A/G (S→S/S/S/S/G)	480	G→G/G/T/G/T (Q→Q/Q/H/Q/H)
	499	A→A/G/A/A/A (I→I/V/I/I/I)	661	T→T/T/T/C/T (Y→Y/Y/Y/H/Y)
	940	G→A/G/G/G/G (A→T/A/A/A/A)	1172	G→A/G/G/G/G (C→Y/C/C/C/C)
	1796	G→A/G/G/G/G (C→Y/C/C/C/C)		
nsp10	329	G→A/G/G/G/G (G→E/G/G/G/G)	719	G→A/G/G/G/G (S→N/S/S/S/S)
	1138	A→T/A/A/A/A (M→L/M/M/M/M)		
nsp11	90	A→A/A/A/A/T (E→E/E/E/E/D)	317	G→G/G/G/A/G (G→G/G/G/D/G)
	584	A→A/A/A/A/C (Q→Q/Q/Q/Q/P)		
nsp12	46	A→A/A/G/A/A (I→I/I/V/I/I)	298	A→A/A/A/G/A (T→T/T/T/A/T)
ORF2a	14	T→C/T/T/T/T (L→P/L/L/L/L)	40	G→G/G/G/A/G (A→A/A/A/T/A)
	148	A→G/A/A/A/A (T→A/T/T/T/T)	497	T→T/T/T/C/T (L→L/L/L/P/L)
	563	A→A/G/G/A/A (D→D/G/G/D/D)		
ORF2b	35	G→G/G/G/A/G (G→G/G/G/D/G)		
ORF3	125	A→G/A/A/A/A (N→S/N/N/N/N)	172	C→C/T/C/C/C (P→P/S/P/P/P)
	173	C→C/C/T/T (P→P/P/P/L/L)	235	C→T/T/C/C/C (H→Y/Y/H/H/H)
	260	A→A/G/G/G/G (H→H/R/R/R/R)[c]	427	T→C/C/C/C/C (F→L/L/L/L/L)[b]
	695	C→C/C/T/C/C (S→S/S/L/S/S)		
ORF5a	38	T→T/T/T/C/T (L→L/L/L/P/L)	119	T→C/C/C/C/C (L→P/P/P/P/P)[b]
ORF5	28	T→T/T/T/C/T (C→C/C/C/R/C)	109	T→C/C/C/C/C (S→P/P/P/P/P)[b]
	177	A→A/A/A/A/T (K→K/K/K/K/N)	280	G→G/G/A/G/G (A→A/A/T/A/A)
	406	T→T/C/C/C/C (Y→Y/H/H/H/H)[c]	554	C→C/T/C/C/T (A→A/V/A/A/V)
ORF6	383	A→G/G/G/G/G (N→S/S/S/S/S)[b]		
ORF7	19	A→A/A/G/A/A (K→K/K/E/K/K)	30	G→G/T/G/G/G (K→K/N/K/K/K)
	266	C→T/C/T/C/C (T→I/T/I/T/T)		

[a] Loci (5′) indicates the nucleotide position on the corresponding gene.
[b] Conserved amino acid mutations among JX-P51, JX-αP51-1, JX-αP51-2, JX-αP51-3 and JX-αP51-4.
[c] Conserved amino acid mutations among JX-αP51-1, JX-αP51-2, JX-αP51-3 and JX-αP51-4.

significance of the variability among different groups by a one-way or two-way ANOVA test of variance. Differences were considered statistically significant at a p-value of < 0.05.

3. Results

3.1. IFNα-resistant PRRSV strains were screened out through serially passaged 45 times in IFNα-treated PAMs

To explore the adaptive mutations of the PRRSV genome under IFNα-induced immune pressure *in vitro*, the HP-PRRSV representative strain JXwn06 was serially passaged 45 times in IFNα-treated PAMs with three independent repeats. Meanwhile, the IFNα-untreated groups were set as controls for monitoring the appearance of mutations that might relate to PAM adaptation. The viruses harvested from each passage were named JX-Pn or JX-αPn (n = 1 to 45) for IFNα-untreated or IFNα-treated viruses, respectively. Viral titers were measured by $TCID_{50}$ assay every 5 passages, and the results showed that the viral titers of the IFNα-treated groups were significantly lower than the titers of the untreated groups during the first 20 passages. However, under IFNα-induced immune pressure, the titers of JX-αPn began to gradually increase after the 25th passage (Fig. 1). After the 45th passage, there was no obvious titer increase in the JX-αPn groups (data not shown), indicating that the IFNα sensitivity of the virus was plateaued at that point. Therefore, the viruses in this passage were used for purification and further evaluation of IFNα sensitivity.

3.2. Four IFNα-resistant PRRSV strains were successfully purified

The passaged viruses, from three independent trials of serial passage in IFNα-treated PAMs, were submitted for three rounds of limited-dilution purification followed by three rounds of serial passaging to

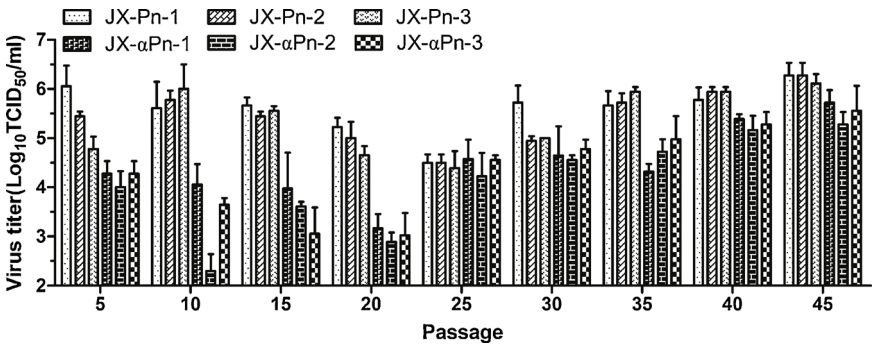

Fig. 1. Viral titers of each passage during serial passaging. The data are shown as the means ± SD of three independent experiments.

increase the quantity of virus. Finally, four strains were purified, named JX-αP51-1, JX-αP51-2, JX-αP51-3 and JX-αP51-4. Among the purified strains, both JX-αP51-2 and JX-αP51-3 were from the same inoculum, and the remaining two strains were from each individual inoculum before purification. The PRRSV control strain passaged without IFNα treatment was named JX-P51.

3.3. Four IFNα-selected PRRSV strains show reduced IFNα sensitivity

To evaluate the IFNα sensitivity of the selected PRRSV strains, the differences in viral growth kinetics in PAMs with or without IFNα (200 U/ml) treatment were analyzed. As shown in Fig. 2A, without exogenous IFNα treatment, four IFNα-selected viruses showed similar growth kinetics as JX-P51 in the PAMs, the peak titers of all viruses reached $10^{6.33}$ to $10^{6.78}$ $TCID_{50}$/ml at 48 hpi. Usually, the mutant virus generated under a selective pressure has a cost in its replication capacity in the absence of this pressure, however there was no obvious viral titer difference observed in the IFNα-untreated PAMs. In the IFNα-treated PAMs, the viral titer of JX-P51 dropped significantly, with a peak titer of $10^{4.55}$ $TCID_{50}$/ml, which was 100-fold lower than its titer in IFNα-untreated PAMs; furthermore, there was a 12 h delay before JX-P51 reaching its peak titer. Conversely, the IFNα-resistant virus reached higher titers than JX-P51, with a significant difference ($p < 0.001$) at almost all time points. The peak titer of JX-αP51-2 reached 10^{6} $TCID_{50}$/ml (Fig. 2B). To clearly show the IFNα sensitivity of different strains, the titer difference of the individual strains between IFNα-treated and untreated conditions was calculated and is displayed in Fig. 2C. JX-P51 was most sensitive to IFNα, with a titer decrease of $10^{2.2}$ $TCID_{50}$/ml at the peak. However, titer differences among the four JX-αP51 strains were smaller, ranging from $10^{0.6}$ to $10^{1.2}$ $TCID_{50}$/ml. These results indicate that four PRRSV strains with reduced IFNα sensitivity were selected by serial passaging in IFNα-treated PAMs.

3.4. IFNα-resistant strains interfere with IFNα-induced transcription of ISGs by disrupting phosphorylation of STAT1/STAT2

IFNα/β signaling induces a potent antiviral state by enhancing the expression of hundreds of ISGs, which are critical for restricting viral infections (Schoggins et al., 2011). To initially analyze the capability of IFNα-selected strains to antagonize IFNα-mediated responses, the transcription levels of two representative ISGs, ISG54 and RNase L, were evaluated by quantitative RT-PCR. As shown in Fig. 3A, the transcription level of ISG54 in mock-infected PAMs was markedly increased 87.5-fold after IFNα stimulation. Meanwhile, PRRSV suppressed mRNA transcription in all inoculation groups ($p < 0.001$), but the ISG54 expression level in IFNα-resistant virus groups was lower than that in JX-P51, with significant differences in strains JX-αP51-1, JX-αP51-2 and JX-αP51-3 ($p < 0.01$, $p < 0.001$ and $p < 0.001$, respectively). Similarly, compared with JX-P51, these three strains also substantially reduced in the RNase L transcription level (Fig. 3B). These results indicate that, compared with the passaging-control strain, the IFNα-resistant PRRSV strains showed a greater capability to antagonize the ISG transcription induced by IFNα.

IFNα acts through binding to the IFNα/β receptor (IFNAR) and activating the JAK-STAT pathway. To determine whether the selected viruses had an increased ability to antagonize the IFNα effect by modulating the STAT1 or STAT2 pathway, the expression level and phosphorylation status of STAT1 or STAT2 in response to IFNα were determined in PRRSV-infected cells. PAMs were infected with PRRSV strains at an MOI of 0.01 for 24 h and then treated with 200 U/ml IFNα for 0.5 h, followed by Western blot. The PAMs without IFNα treatment were used as the mock control. As shown in Fig. 3C, the protein expression levels of STAT1 and STAT2 were similar in all groups, but the phosphorylation status of these two proteins varied. The basal expression levels of pSTAT1 and pSTAT2 in untreated mock cells were very low, and the amount of pSTAT2 was below the detection limit. After IFNα stimulation, the expression levels of both pSTAT1 and pSTAT2 were markedly increased in uninfected PAMs. Correspondingly,

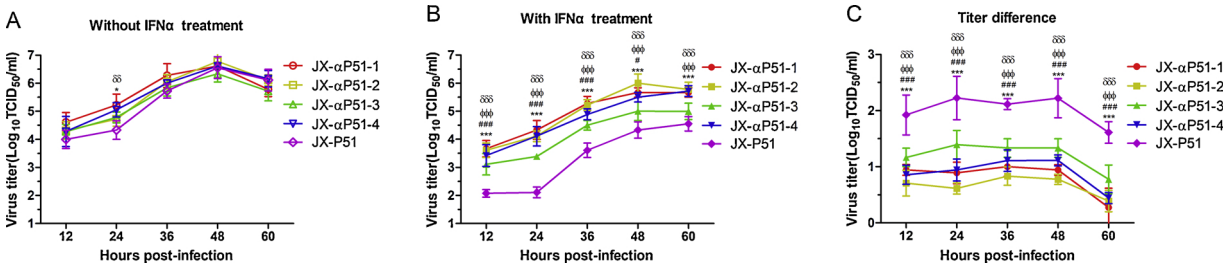

Fig. 2. The growth kinetics and IFNα sensitivity of viruses selected in PAMs by IFNα treatment. (A and B) PAMs were not treated or treated with IFNα (200 U/ml) for 24 h and then infected with the indicated PRRSV strains at an MOI of 0.01 and maintained under conditions without or with IFNα (200 U/ml). The cultures were collected at different time points post-infection and titrated. (C) Reduction of viral titers between treatments with and without exogenous IFNα. Delta (δ), phi (ϕ), pound (#) and asterisks (*) indicate a significant difference in the viral titers between IFNα-resistant virus (JX-αP51-1, JX-αP51-2, JX-αP51-3 and JX-αP51-4, respectively) and JX-P51 (*** $p < 0.001$, ** $p < 0.01$ and * $p < 0.05$). The data are shown as the means ± SD of three independent experiments.

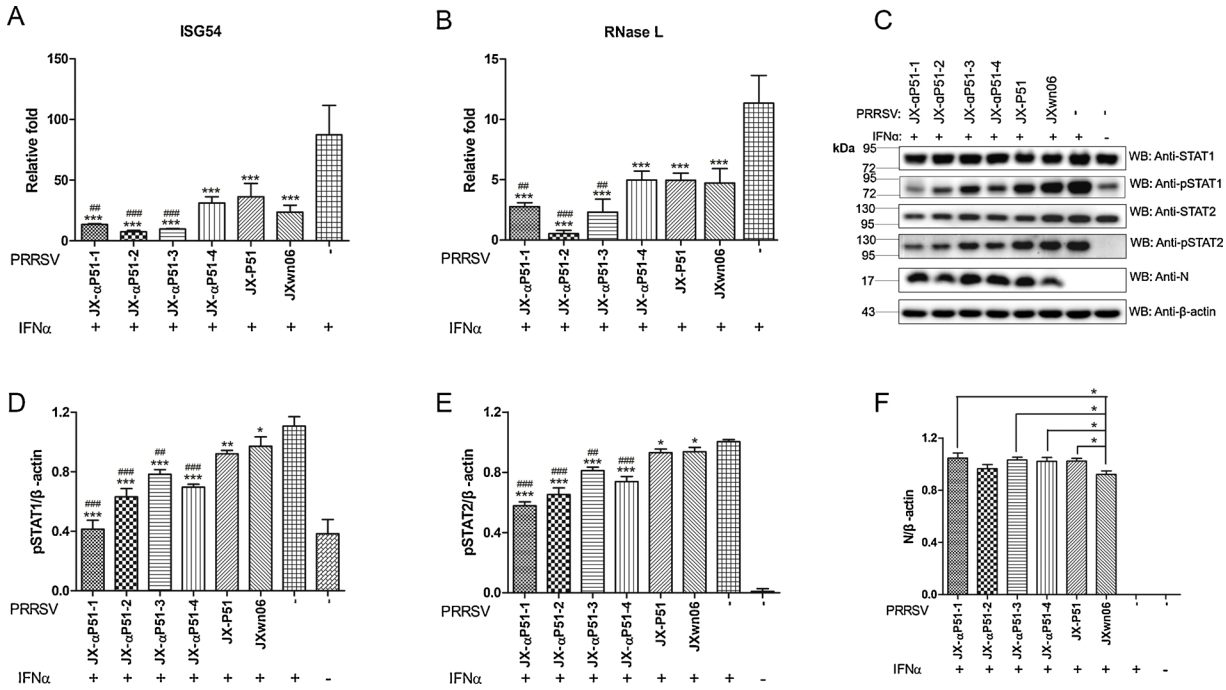

Fig. 3. Downregulation of IFNα-activated cellular expression of ISGs and phosphorylation of cellular STAT1 and STAT2 by PRRSV infection. (A) and (B) Downregulation of IFNα-induced ISG transcription by PRRSV infection. PAMs were inoculated with the indicated PRRSV strain at an MOI of 0.01 for 24 h and then treated with IFNα (200 U/ml) for 8 h. The transcription level of the two ISGs were analyzed by qRT-PCR. The relative fold change is shown in comparison with cells with neither IFNα treatment nor PRRSV inoculation. (C) PRRSV infection inhibits IFNα-induced phosphorylation of cellular STAT1 and STAT2. PAMs were infected with indicated PRRSV strains at an MOI of 0.01. At 24 h post-infection, the cells were treated with IFNα for 0.5 h, then the expression levels of STAT1, STAT2, viral N protein and β-actin, as well as the level of phosphorylated STAT1 (pSTAT1) and phosphorylated STAT2 (pSTAT2) were determined by Western blot. The optical density ratios of pSTAT1/β-actin (D), pSTAT2/β-actin (E) and N/β-actin (F) were analyzed by Image Studio. The data are shown as the means ± SD of three independent experiments and the significant differences were analyzed by using a two-way RM ANOVA in the GraphPad Prism (version 5.0). From (A) to (E), the asterisk (*) indicates a significant difference in the mRNA or protein expression level between the indicated group and IFNα-treated noninfected PAMs (*** $p < 0.001$, ** $p < 0.01$ and * $p < 0.05$); and the pound (#) indicates a significant difference in the mRNA or protein expression level between the indicated group and JX-P51-infected PAMs (### $p < 0.001$, ## $p < 0.01$ and # $p < 0.05$), respectively. In (F), the asterisk (*) indicates a significant difference in the viral N protein level between indicated two groups (* $p < 0.05$).

JXwn06 or JX-P51 infection both resulted in inhibition of STAT1/STAT2 phosphorylation, with significant differences ($p < 0.05$) compared with non-infection group. Moreover, the levels of pSTAT1 and pSTAT2 were notably lower in PAMs infected with IFNα-resistant viruses, with significant differences ($p < 0.001$) (Fig. 3D and 3E). The expression levels of STAT1 and STAT2 were not affected by any viral infection (Fig. 3C), indicating that losses of pSTAT1 and pSTAT2 did not result from a decrease in STAT1/STAT2 expression or increase in specific protein degradation. Considering the similar level of viral N protein among the IFNα-resistant and passaging-control viruses (Fig. 3F), it is worth noting that the pSTAT1 and pSTAT2 variation was not related to the viral titer difference but was related to the capability of the IFNα-resistant virus to inhibit the phosphorylation of STAT1 and STAT2.

3.5. IFNα-resistant virus inhibits JAK1 activation by suppressing its phosphorylation

To further identify the suppressing target, upstream of pSTAT1 and pSTAT2, the expression levels of JAK1 and phosphorylated JAK1 were investigated as above. As shown in Fig. 4A, the expression level of JAK1 was similar in all groups, but the phosphorylation of JAK1 was undetectable in untreated control cells. After IFNα stimulation, the levels of phosphorylated JAK1 (pJAK1) in PAMs increased in mock-infected cells, but the infection with IFNα-resistant virus could greatly reduce the level of pJAK1 compared with the PAMs infected with JX-P51 or wild-type JXwn06 (Fig. 4A and 4B). The inhibition effect required viral replication, as it disappeared if the virus was inactivated by UV irradiation prior to inoculation (Fig. 4C). Moreover, this virus-mediated inhibition of JAK1 phosphorylation could be eliminated by treatment with the tyrosine phosphatase inhibitor Na_3VO_4 in a dose-dependent manner (Fig. 4D and 4E). Furthermore, the expression levels of IFNα receptors IFNAR1 and IFNAR2, the upstream activators of JAK1, were similar in all groups (Fig. 4F).

These results demonstrated that IFNα-resistant PRRSVs could suppress the JAK-STAT activation pathway by counteracting JAK1 phosphorylation through tyrosine phosphatase-mediated dephosphorylation.

3.6. The conserved mutant sites among all passaged strains or IFNα-resistant strains were identifited

To identify the genetic variation among IFNα-resistant viruses that contributes to the increased IFNα antagonistic capability, the full-length genomic sequences of 4 IFNα-resistant mutant strains as well as JX-P51 were obtained and aligned with the genomic sequence of wild-type JXwn06. The variations were dispersed throughout the genome, with the exception of nsp6 and nsp8, which are two short conserved coding regions; however, there were no nucleotide deletions or insertions present in all 5 strains. The amino acid residue mutation and their locations are summarized in Table 2. In addition, nsp1β (E87 G), GP3 (F143 L), GP5a (L40 P), GP5 (S37 P) and M (N128S) were conserved in all 5 passaged strains, and GP3 (H87R) and GP5 (Y136 H) were only conserved in IFNα-resistant viruses.

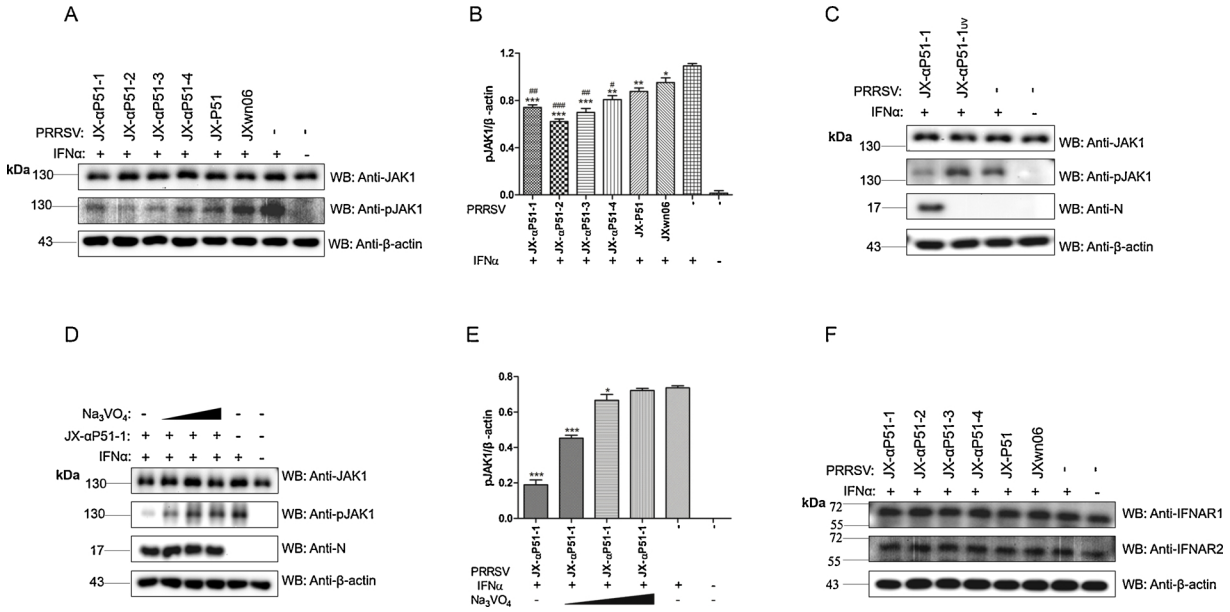

Fig. 4. PRRSV infection results in decreased phosphorylation of JAK1 in IFNα-treated PAMs without affecting the expression levels of IFNAR1 and IFNAR2. (A, B and C) PAMs were inoculated with the indicated PRRSV strains or UV-inactivated JX-αP51-1 at an MOI of 0.01 for 24 h and then treated with IFNα (200 U/ml) for 0.5 h. Then, cell lysates were analyzed by Western blot with antibodies against JAK1 and pJAK1, and cells without IFNα treatment served as the controls. pJAK1 protein bands were quantitated for 3 repeated assays using Image Studio software and normalized to β-actin. The data are shown as the means ± SD. The asterisk (*) indicates a significant difference in pJAK1 expression levels between PRRSV-infected and mock-infected PAMs (*** $p < 0.001$, ** $p < 0.01$ and * $p < 0.05$). Pound (#) indicates a significant difference compared with JX-P51-infected PAMs (### $p < 0.001$ and # $p < 0.05$). The data are shown as the means ± SD. (D and E) PAMs were challenged with JX-αP51-1 at an MOI of 0.01. The cells at 20 hpi were treated with increasing doses of Na_3VO_4 (0 μM, 100 μM, 200 μM and 300 μM) for 4 h, followed by IFNα treatment or not for 0.5 h and were then subjected to Western blot with anti-pJAK1, anti-JAK1, anti-N, or anti-β-actin antibodies. The relative fold changes of the optical density ratios of pJAK1/β-actin are shown. Data are shown as the means ± SD of three independent experiments (*** $p < 0.001$ and ** $p < 0.05$). (F) IFNAR1 or IFNAR2 expression levels were examined by Western blot with antibodies against IFNAR1 or IFNAR2.

3.7. The mutations of nsp1β (E87 G), GP3 (F143 L) and GP5 (Y136 H) were identified to correlate with increased IFNα resistance

To explore the mutation(s) that might be responsible for the reduced IFNα sensitivity of the viruses, 6 strains each containing each one of the conserved amino acid mutations mentioned above were constructed and rescued by using pWSK-JXwn as the backbone (Table 3). Considering that both mutations in GP5a (L40 P) and GP5 (S37 P) were caused by the same nucleotide site substitution, to simplify the name of this strain, only residue 37 of GP5 is mentioned in the following study. The IFNα sensitivities of these mutant strains were analyzed relative to their parental backbone virus RvJXwn using the method described above. In the IFNα-untreated PAMs, two strains, RvJX_nsp1β-E87 G and RvJX_GP3-F143 L, showed increased replication efficiency, with significantly higher titers than RvJXwn at 12, 24, and 36 hpi ($p < 0.05$) or from 12 to 48 hpi ($p < 0.05$), respectively. In addition, RvJX_GP5-S37 P had a higher titer only at 36 hpi ($p < 0.01$), and the rest of the strains showed similar growth characteristics as the backbone virus (Fig. 5A). Most notably, in another study of our lab, the GP3 (F143 L) mutation was also found in the strain that was serially propagated in PAMs with treatment of PRRSV neutralizing antibody (unpublished data, that will be used for another article). It indicates that this site mutation might be also related with PRRSV adaptation to PAMs and the improved IFN-resistance might be more or less benefit for its replication, even in the PAMs without treatment of exogenous IFNα. In the IFNα-treated PAMs, the replication of the backbone virus RvJXwn was markedly suppressed, showing very low titers, but RvJX_nsp1β-E87 G, RvJX_GP3-F143 L and RvJX_GP5-Y136H, especially the first two strains, grew well (Fig. 5B). The titers of RvJXwn in IFNα-treated PAMs were approximately 2–3.5 logs lower than the titers in untreated PAMs, but for RvJX_nsp1β-E87 G and RvJX_GP3-F143 L, the titer difference in IFNα-treated or untreated PAMs was close to 1 log (Fig. 5C). The remaining mutated viruses showed similar IFNα sensitivity as their backbone virus RvJXwn.

The results above indicated that the mutations of nsp1β (E87 G), GP3 (F143 L) and GP5 (Y136 H) correlated with increased IFNα resistance in the selected virus, and substitutions of nsp1β (E87 G) and GP3 (F143 L) might contribute more to the IFNα resistance than GP5

Table 3
The list of rescued viruses with mutated respective amino acid sites.

Name	Abbreviated name	Mutations
RvJX_n1β-E87G	n1β-E87G	nsp1β (E87 G)
RvJX_GP3-H87R	GP3-H87R	GP3 (H87R)
RvJX_GP3-F143 L	GP3-F143L	GP3 (F143 L)
RvJX_GP5-S37P	GP5-S37P	GP5 (S37 P)
RvJX_GP5-Y136H	GP5-Y136H	GP5 (Y136 H)
RvJX_M-N128S	M-N128S	M (N128S)
RvJX-C1	JX-C1	GP3 (H87R) and GP5 (Y136 H)
RvJX-C2	JX-C2	nsp1β (E87 G), GP3 (F143 L), GP5 (S37 P) and M (N128S)
RvJX-C3	JX-C3	GP3 (H87R), GP3 (F143 L), GP5 (S37 P), GP5 (Y136 H) and M (N128S)
RvJX-C4	JX-C4	nsp1β (E87 G), GP3 (H87R), GP3 (F143 L), GP5 (S37 P), GP5 (Y136 H) and M (N128S)

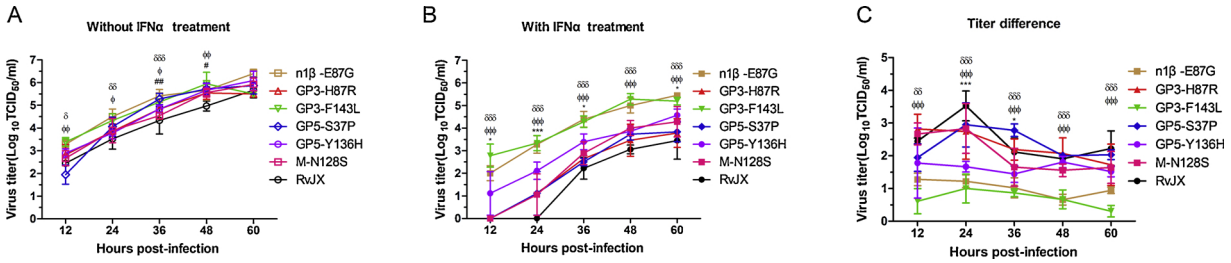

Fig. 5. Identification of the mutation sites correlated with IFNα resistance. The growth kinetics of the rescued viruses in PAMs without (A) or with (B) IFNα (200 U/ml) treatment. (C) Reduction of viral titers between treatments without and with exogenous IFNα. Delta (δ), phi (ϕ), pound (#) and asterisk (*) indicate a significant difference in the viral titers between mutated viruses (RvJX_n1β-E87 G, RvJX_GP3-F143 L, RvJX_GP5-S37 P and RvJX_GP5-Y136H, respectively) and RvJXwn (*** $p < 0.001$, ** $p < 0.01$ and * $p < 0.05$). Data are shown as the means ± SD of three independent experiments.

(Y136 H).

3.8. Three mutations contribute to the increased capability of the virus to block the IFNα-activated JAK-STAT signaling pathway

To elucidate the role of the mutations at nsp1β (E87 G), GP3 (F143 L) and GP5 (Y136 H), in IFNα resistance, the expression level and phosphorylation status of JAK1, STAT1 and STAT2 were examined in IFNα-treated PAMs infected with the various PRRSV mutant strains (Table 3). After IFNα treatment, the levels of pJAK1, pSTAT1 and pSTAT2 were lower in all PRRSV-infected PAMs than in mock-infected cells. Consistent with the IFNα sensitivity above, the levels of pJAK1, pSTAT1 and pSTAT2 were much lower in the PAMs infected with RvJX_nsp1β-E87 G, RvJX_GP3-F143 L or RvJX_GP5-Y136H compared with the levels in RvJXwn and the rest of the single site mutant viruses (RvJX_GP3-H87R, RvJX_GP5-S37 P and RvJX_M-N128S). The inhibition effect was more obvious when the virus harbored more than one of the nsp1β (E87 G), GP3 (F143 L) and GP5 (Y136 H) substitutions, as the phosphorylation level of JAK1 in JX-C3- or JX-C4-infected groups was even lower (Fig. 6).

The JAK-STAT signaling pathway data further demonstrated that substitutions at nsp1β (E87 G), GP3 (F143 L) and GP5 (Y136 H) conferred increased IFNα resistance to the selected viruses.

4. Discussion

The IFN system plays an important role in host defense against viral infection by direct antiviral effects, as well as through immune regulation to link innate and adaptive immune responses (Stetson and Medzhitov, 2006). To evade host antiviral immunity, viruses have evolved multiple strategies to antagonize IFN by disrupting its induction, signaling or functions (Garcia-Sastre, 2017). Earlier studies demonstrated evidence of the relationship between IFN phenotypes and viral virulence or infection persistence (Carrigan and Knox, 1990). Numerous studies have confirmed that PRRSV could interact with the host IFN system, leading to a weakened host antiviral response, as several virus-encoded proteins have been identified as antagonists of IFN induction or downstream signaling. On the other hand, PRRSV is characterized by genetic, antigenic and pathogenic variability among field strains, including diverse IFN phenotypes. Notably, the induction of and sensitivity to IFN not only differ among various PRRSV isolates but also show variation among the plaque-derived populations within each isolate (Lee et al., 2004). The diversity of IFN sensitivity indicates that IFN might act as a selective pressure to drive viral evolution toward developing IFN resistance. To investigate this hypothesis and explore the genetic variation of the virus during adaptation to IFN-treated host cells, in the present study, PRRSV was serially passaged in PAMs with exogenous IFNα in the culture medium to artificially accelerate the evolutionary process. After 45 passages in PAMs and 3 rounds of plaque purification, four strains of virus with increased IFNα resistance were selected out.

Generally, one of the major anti-virus effect of IFN is to inhibit the replication of virus, so the impact of exogenous IFNα treatment on the viral growth characterization in the PAMs were used to evaluate the viral IFNα sensitivity in this study. As expected, in the presence of exogenous IFNα in the PAMs, the IFNα-selected strains showed less viral titers reduction, compared with the non-selected virus, indicating the increased IFNα resistance. Meanwhile, without exogenous IFNα treatment, four IFNα-selected viruses showed similar growth kinetics with that of unselected one, revealing that IFNα-selecting pressure did not obviously change the viral replication capability in the PAMs without exogenous IFNα treatment. Host cells employ the IFN system as an important line of defense against viral infections, correspondingly, PRRSV could interfere in IFN induction and function to create a suitable environment for its replication, and the resistance to IFN might be more or less benefit for viral growth on PAMs. This explained why the mutations generated under the IFNα-selecting pressure did not have a cost in the viral replication capacity in the absence of this pressure.

The IFN-activated JAK-STAT signaling pathway is significant for the immune response, which is often targeted by pathogens, such as PRRSV, to suppress the host defense. PRRSV has been found to interfere with interferon-activated JAK-STAT signaling through several strategies. For example, PRRSV infection can upregulate host suppressive signals, including miR-30C, and suppressors of cytokine signaling (SOCS) proteins to antagonize the JAK-STAT pathway (Wysocki et al., 2012; Zhang et al., 2016). Additionally, PRRSV nsp1β inhibits the nuclear translocation of interferon-stimulated gene factor 3 (ISGF-3) by inducing degradation of karyopherin α1 (KPNA1), which is a critical adaptor in nucleocytoplasmic transport (Wang et al., 2013a). The PRRSV N protein also inhibits ISGF-3 nuclear translocation (Patel et al., 2010). To determine the mechanism of the increased IFNα resistance of these mutant viruses, the IFNα-stimulated JAK-STAT signaling pathway was investigated in PRRSV-infected PAMs. Interestingly, the results clearly indicated that all tested PRRSV strains could inhibit IFN-activated phosphorylation of STAT1 and STAT2. In particular, phosphorylation of STAT1 and STAT2 was even lower in the IFNα-resistant strains-infected cells. This finding is different from a previous study by Patel (2010) which indicated that PRRSV is involved in blocking nuclear translocation of pSTAT1 and pSTAT2 without affecting IFN-induced phosphorylation of STAT1/STAT2 (Patel et al., 2010). However, a study from Chen (2010) showed that PRRSV could inhibit IFNβ-activated phosphorylation of STAT1 via nsp1β (Chen et al., 2010). This discrepancy may be due to the use of different virus strains and IFN subtypes (Yang and Zhang, 2017), but it still requires further investigation.

In the IFNα-induced JAK-STAT signaling pathway, the phosphorylation of STAT1 and STAT2 requires the upstream activation of JAK1 and TYK2. The experiments in this study showed that PRRSV inhibited IFNα-mediated signaling by reducing the phosphorylation of JAK1 upon IFNα treatment, with no effect on the total protein level of JAK1 (Fig. 4A). In addition, the UV-inactivated PRRSV was deficient in inhibiting phosphorylation of JAK1 (Fig. 4C). Furthermore, the

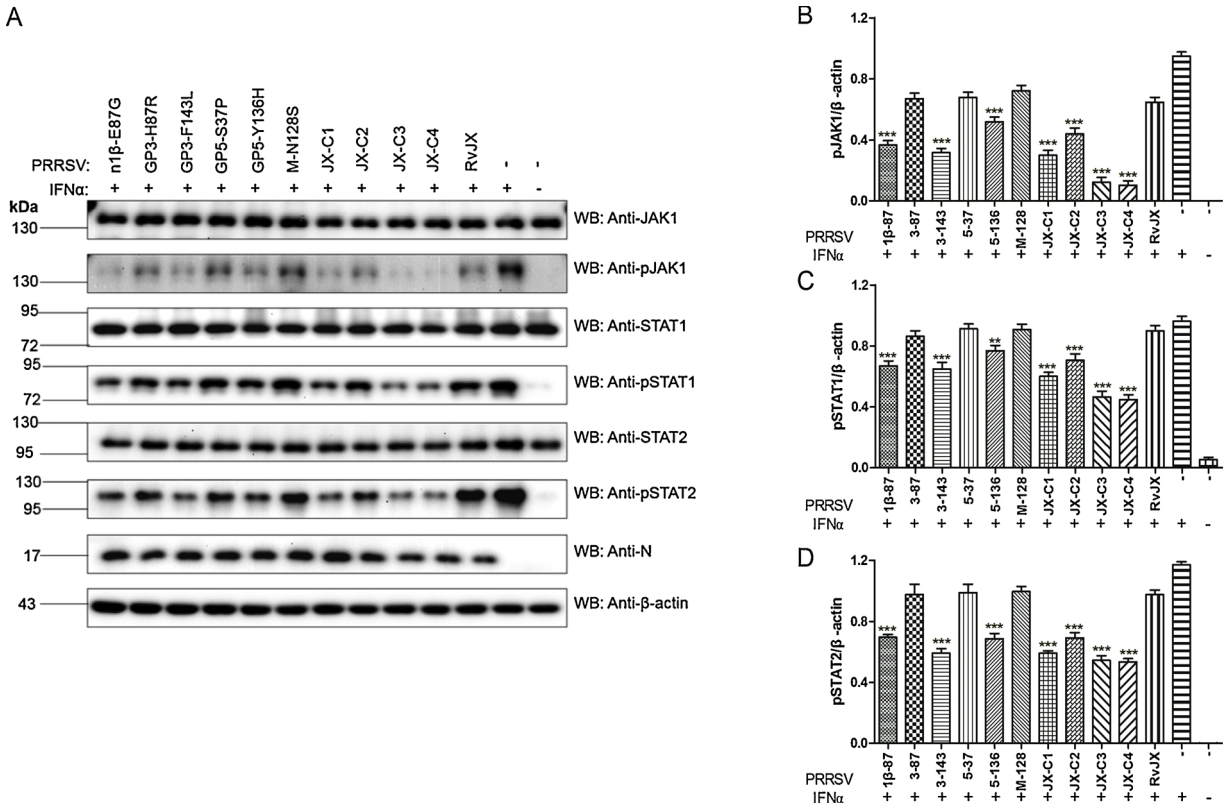

Fig. 6. Identification of the mutation sites correlated with increased antagonization of the JAK-STAT signaling pathway. (A) PAMs were infected with mutant viruses at an MOI of 0.01 for 24 h or left uninfected and then not treated or treated with IFNα (200 U/ml) for 0.5 h. All of the cells were subjected to Western blot to determine the expression of JAK1, STAT1, STAT2, N and β-actin, as well as the level of pJAK1, pSTAT1 and pSTAT2. JX-C1 contains GP3 (H87R) and GP5 (Y136 H) mutations; JX-C2 contains nsp1β (E87 G), GP3 (F143 L), GP5 (S37 P), and M (N128S) mutations; JX-C3 carries all conserved mutations except for nsp1β (E87 G); and JX-C4 contains all conserved mutations mentioned above. (B) pJAK1, pSTAT1 and pSTAT2 protein bands were quantitated for three repeated assays using Image Studio software and normalized to β-actin. Data are shown as the means ± SD (*** $p < 0.001$, ** $p < 0.01$, * $p < 0.05$).

expression levels of IFNAR1 and IFNAR2, two upstream activating molecules of JAK1, were similar in all infected groups (Fig. 4F). Importantly, the PRRSV-induced reduction of JAK1 phosphorylation could be eliminated by sodium orthovanadate, a phosphatase inhibitor, in a dose-dependent manner (Fig. 4D and 4E), which indicated that pJAK1 is downregulated by the induced dephosphorylation of JAK1 by PTPs. Therefore, the other negative regulators, including suppressors of cytokine signaling (SOCS) and protein inhibitor of activated STATs (PIAS) (Morris et al., 2018), were not further examined in this study. However, in contrast to our results, recent reports from another group showed that PRRSV upregulates host miR-30c, which negatively regulates IFNα/β signaling by targeting JAK1 and IFNAR2, to facilitate PRRSV replication (Liu et al., 2018; Zhang et al., 2016). Considering that the MOI used in our study was different from that of the conflicting report, we increased the virus MOI to the same level reported as Zhang (2016) and found that the expression level of JAK1 was downregulated by JXwn06 at 24 hpi at an MOI of 1 (data not shown). In addition, Zhang (2018) conducted a quantitative proteomic approach with a label-free quantitative method to analyze changes in the ubiquitination level in PRRSV-infected PAMs and found that level of ubiquitinated JAK1 could be changed during PRRSV inoculation, leading to a significant reduction of JAK1 (Zhang et al., 2018). These findings imply that PRRSV has multiple strategies to block the JAK-STAT signaling pathway and promoting JAK1 dephosphorylation (observed in this study) is one of the many strategies.

The PRRSV genetic variation under selective pressure from IFNα was determined via full genomic sequencing and alignment. As expected, the variation sites were distributed throughout the genome, so, it can't directly find out the amino acid substitution related to IFNα resistance only based on the sequencing data, which complicated the identification of IFNα-correlated mutation(s). But it provided a clue for narrowing down the search range, and the contribution of these substitutions to IFNα resistance could be further confirmed by the reverse genetic operation. Two mutation sites GP3 (H87R) and GP5 (Y136 H) conserved among the four IFNα-resistant strains were initially analyzed. Theoretically, these sites might be more likely to contribute to the resistance. Additionally, four mutation sites conserved among all passaged viruses were also investigated, as they might relate to PAM adaptation or they might contribute to the IFNα resistance by interacting with other sites. Our IFNα sensitivity evaluation and Western blot data revealed that the substitutions at nsp1β (E87 G), GP3 (F143 L) and GP5 (Y136 H) led to higher IFNα resistance via increased antagonization of JAK1 phosphorylation, and the antagonistic effect was increased when the three sites were combined (Fig. 6A). Among these three sites, nsp1β (E87 G) and GP3 (F143 L) exist in all passaged viruses, including JX-P51, the virus passaged without exogenous IFN selection. It is easy to raise a concern, why they do not lead to the improvement of IFN-α resistance when they exist in JX-P51. Their contribution to the increased IFN-α resistance were identified through mono-factor analysis (site mutation) by comparing the site (s) mutant virus with their backbone parental virus. But for the virus JX-P51, there are still lots of mutations distributed among the whole genome, some of which might interrupt the function of mutated sites nsp1β (E87 G) and GP3 (F143 L) in it. We aligned 540 field strains of type 2 PRRSV to analyze the distribution of these three sites, and the results showed that only one strain (KU131563_SD98-163-P83) has residue G at position 87 of nsp1β, and another strain (KF287134_HK4) has residue H at position 136 of GP5; however, 207 strains have residue L at position 143 of GP3. SD98-163-P83 and HK4 were isolated in the United States in 1998 and Hong Kong in 2003, respectively; however, there is no available

information about their IFN phenotype and virulence. The 207 strains with residue L at position 143 of GP3 could be divided into HP-PRRSV-like strains, classical PRRSV strains, NADC30-like strains and MLV-like strains, demonstrating that there is no direct evidence to link the Leu residue at amino acid 143 of GP3 with viral virulence.

In a previous report, a substitution at nsp1β (I19 V) of the MLV vaccine strain led to it gaining the ability to induce KPNA1 degradation and change its IFNα sensitivity (Wang et al., 2013a). Although three mutation sites correlating with IFNα resistance were identified, we could not rule out the role of other noncommon mutations in antagonizing IFNα activity. In addition, whether these mutations act alone or interact with other viral proteins or host proteins to disturb IFNα signaling requires further investigation.

5. Conclusions

The data presented in this study illustrate that the IFNα resistance of PRRSV can be increased through serial passaging in PAMs under selective pressure from IFNα. The IFNα-resistant virus gained an increased capability to antagonize IFNα signaling by reducing the phosphorylation level of JAK1. Moreover, mutations at nsp1β (E87 G), GP3 (F143 L) and GP5 (Y136 H) in PRRSV were found to correlate with the increased capability of the virus to antagonize JAK1 phosphorylation. These findings provide additional evidence for understanding PRRSV genetic variation under host selective pressure and viral evolution strategies to evade host innate immunity.

Declaration of Competing Interest

The authors declare that there is no conflict of interest.

Acknowledgments

This study was supported by the Major program of National Natural Science Foundation of China (31490603), the National Key Technology R & D Program of China from the Chinese Ministry of Science and Technology (2015BAD12B01-2), and the National Natural Science Foundation of China (31772759).

References

Albina, E., 1997. Epidemiology of porcine reproductive and respiratory syndrome (PRRS): an overview. Vet. Microbiol. 55, 309–316.

Buddaert, W., Van Reeth, K., Pensaert, M., 1998. *In vivo* and *in vitro* interferon (IFN) studies with the porcine reproductive and respiratory syndrome virus (PRRSV). Adv. Exp. Med. Biol. 440, 461–467.

Calzada-Nova, G., Schnitzlein, W.M., Husmann, R.J., Zuckermann, F.A., 2011. North American porcine reproductive and respiratory syndrome viruses inhibit type I interferon production by plasmacytoid dendritic cells. J. Virol. 85, 2703–2713.

Carrigan, D.R., Knox, K.K., 1990. Identification of interferon-resistant subpopulations in several strains of measles virus: positive selection by growth of the virus in brain tissue. J. Virol. 64, 1606–1615.

Chen, Z., Lawson, S., Sun, Z., Zhou, X., Guan, X., Christopher-Hennings, J., Nelson, E.A., Fang, Y., 2010. Identification of two auto-cleavage products of nonstructural protein 1 (nsp1) in porcine reproductive and respiratory syndrome virus infected cells: nsp1 function as interferon antagonist. Virology. 398, 87–97.

Dong, H., Zhou, L., Ge, X., Guo, X., Han, J., Yang, H., 2018. Porcine reproductive and respiratory syndrome virus nsp1beta and nsp11 antagonize the antiviral activity of cholesterol-25-hydroxylase via lysosomal degradation. Vet. Microbiol. 223, 134–143.

Fang, Y., Treffers, E.E., Li, Y., Tas, A., Sun, Z., van der Meer, Y., de Ru, A.H., van Veelen, P.A., Atkins, J.F., Snijder, E.J., Firth, A.E., 2012. Efficient -2 frameshifting by mammalian ribosomes to synthesize an additional arterivirus protein. Proc. Natl. Acad. Sci. U. S. A. 109, E2920–2928.

Garcia-Sastre, A., 2017. Ten strategies of interferon evasion by viruses. Cell Host Microbe 22, 176–184.

Han, J., Zhou, L., Ge, X., Guo, X., Yang, H., 2017. Pathogenesis and control of the Chinese highly pathogenic porcine reproductive and respiratory syndrome virus. Vet. Microbiol. 209, 30–47.

He, D., Niu, X., Jiang, A., Su, D., Zhong, W., Hu, J., Wang, Y., Chen, R., 2013. swIFN-beta promotes genetic mutation of porcine reproductive and respiratory syndrome virus in MARC-145. Vet. Microbiol. 166, 174–178.

He, W., Wei, Y., Yao, J., Xie, X., Huang, J., Lin, S., Ouyang, K., Chen, Y., Huang, W., Wei, Z., 2018. Effect of an 88-amino-acid deletion in nsp2 of porcine reproductive and respiratory syndrome virus on virus replication and cytokine responses in vitro. Arch. Virol. 163, 1489–1501.

Keffaber, K., 1989. Reproductive failure of unknown etiology. Am. Assoc. Swine. Pract. Newsletter. 1, 1–9.

Kuhn, J.H., Lauck, M., Bailey, A.L., Shchetinin, A.M., Vishnevskaya, T.V., Bao, Y., Ng, T.F., LeBreton, M., Schneider, B.S., Gillis, A., Tamoufe, U., Diffo Jle, D., Takuo, J.M., Kondov, N.O., Coffey, L.L., Wolfe, N.D., Delwart, E., Clawson, A.N., Postnikova, E., Bollinger, L., Lackemeyer, M.G., Radoshitzky, S.R., Palacios, G., Wada, J., Shevtsova, Z.V., Jahrling, P.B., Lapin, B.A., Deriabin, P.G., Dunowska, M., Alkhovsky, S.V., Rogers, J., Friedrich, T.C., O'Connor, D.H., Goldberg, T.L., 2016. Reorganization and expansion of the nidoviral family Arteriviridae. Arch. Virol. 161, 755–768.

Lee, S.M., Schommer, S.K., Kleiboeker, S.B., 2004. Porcine reproductive and respiratory syndrome virus field isolates differ in *in vitro* interferon phenotypes. Vet. Immunol. Immunopathol. 102, 217–231.

Li, Y., Zhou, L., Zhang, J., Ge, X., Zhou, R., Zheng, H., Geng, G., Guo, X., Yang, H., 2014. Nsp9 and nsp10 contribute to the fatal virulence of highly pathogenic porcine reproductive and respiratory syndrome virus emerging in China. PLoS Pathog. 10, e1004216.

Liu, F., Wang, H., Du, L., Wei, Z., Zhang, Q., Feng, W.H., 2018. MicroRNA-30c targets the interferon-alpha/beta receptor beta chain to promote type 2 PRRSV infection. J. Gen. Virol. 99, 1671–1680.

Lunney, J.K., Fang, Y., Ladinig, A., Chen, N., Li, Y., Rowland, B., Renukaradhya, G.J., 2016. Porcine reproductive and respiratory syndrome virus (PRRSV): pathogenesis and interaction with the immune system. Annu. Rev. Anim. Biosci. 4, 129–154.

Meng, X.J., Paul, P.S., Halbur, P.G., Lum, M.A., 1996. Characterization of a high-virulence US isolate of porcine reproductive and respiratory syndrome virus in a continuous cell line, ATCC CRL11171. J. Vet. Diagn. Invest. 8, 374–381.

Morris, R., Kershaw, N.J., Babon, J.J., 2018. The molecular details of cytokine signaling via the JAK-STAT pathway. Protein Sci. 27, 1984–2009.

Patel, D., Nan, Y.C., Shen, M.Y., Ritthipichai, K., Zhu, X.P., Zhang, Y.J., 2010. Porcine reproductive and respiratory syndrome virus inhibits type I interferon signaling by blocking STAT1/STAT2 nuclear translocation. J. Virol. 84, 11045–11055.

Schoggins, J.W., Wilson, S.J., Panis, M., Murphy, M.Y., Jones, C.T., Bieniasz, P., Rice, C.M., 2011. A diverse range of gene products are effectors of the type I interferon antiviral response. Nature. 472, 481–485.

Snijder, E.J., Kikkert, M., Fang, Y., 2013. Arterivirus molecular biology and pathogenesis. J. Gen. Virol. 94, 2141–2163.

Stetson, D.B., Medzhitov, R., 2006. Type I interferons in host defense. Immunity. 25, 373–381.

Sun, Z., Li, Y., Ransburgh, R., Snijder, E.J., Fang, Y., 2012. Nonstructural protein 2 of porcine reproductive and respiratory syndrome virus inhibits the antiviral function of interferon-stimulated gene 15. J. Virol. 86, 3839–3850.

Wang, R., Nan, Y., Yu, Y., Zhang, Y.J., 2013a. Porcine reproductive and respiratory syndrome virus nsp1 beta inhibits interferon-activated JAK-STAT signal transduction by inducing karyopherin-alpha 1 degradation. J. Virol. 87, 5219–5228.

Wang, R., Nan, Y.C., Yu, Y., Yang, Z.Q., Zhang, Y.J., 2013b. Variable interference with interferon signal transduction by different strains of porcine reproductive and respiratory syndrome virus. Vet. Microbiol. 166, 493–503.

Wysocki, M., Chen, H., Steibel, J.P., Kuhar, D., Petry, D., Bates, J., Johnson, R., Ernst, C.W., Lunney, J.K., 2012. Identifying putative candidate genes and pathways involved in immune responses to porcine reproductive and respiratory syndrome virus (PRRSV) infection. Anim. Genet. 43, 328–332.

Xiong, Z., Niu, X., Song, Y., Su, D., Wang, F., Chen, R., He, D., 2015. Evolution of porcine reproductive and respiratory syndrome virus GP5 and GP3 genes under swIFN-beta immune pressure and interferon regulatory factor-3 activation suppressed by GP5. Res. Vet. Sci. 101, 175–179.

Xu, L., Zhou, L., Sun, W., Zhang, P., Ge, X., Guo, X., Han, J., Yang, H., 2018. Nonstructural protein 9 residues 586 and 592 are critical sites in determining the replication efficiency and fatal virulence of the Chinese highly pathogenic porcine reproductive and respiratory syndrome virus. Virology. 517, 135–147.

Yang, L., Zhang, Y.J., 2017. Antagonizing cytokine-mediated JAK-STAT signaling by porcine reproductive and respiratory syndrome virus. Vet. Microbiol. 209, 57–65.

Zhang, H., Fang, L., Zhu, X., Wang, D., Xiao, S., 2018. Global analysis of ubiquitome in PRRSV-infected pulmonary alveolar macrophages. J. Proteomics 184, 16–24.

Zhang, H., Guo, X., Ge, X., Chen, Y., Sun, Q., Yang, H., 2009. Changes in the cellular proteins of pulmonary alveolar macrophage infected with porcine reproductive and respiratory syndrome virus by proteomics analysis. J. Proteome Res. 8, 3091–3097.

Zhang, Q., Huang, C., Yang, Q., Gao, L., Liu, H.C., Tang, J., Feng, W.H., 2016. MicroRNA-30c modulates type I IFN responses to facilitate porcine reproductive and respiratory syndrome virus infection by targeting JAK1. J. Immunol. 196, 2272–2282.

Zhao, M., Wan, B., Li, H., He, J., Chen, X., Wang, L., Wang, Y., Xie, S., Qiao, S., Zhang, G., 2017. Porcine 2′, 5′-oligoadenylate synthetase 2 inhibits porcine reproductive and respiratory syndrome virus replication in vitro. Microb. Pathog. 111, 14–21.

Zhou, L., Chen, S., Zhang, J., Zeng, J., Guo, X., Ge, X., Zhang, D., Yang, H., 2009a. Molecular variation analysis of porcine reproductive and respiratory syndrome virus in China. Virus Res. 145, 97–105.

Zhou, L., Zhang, J., Zeng, J., Yin, S., Li, Y., Zheng, L., Guo, X., Ge, X., Yang, H., 2009b. The 30-amino-acid deletion in the nsp2 of highly pathogenic porcine reproductive and respiratory syndrome virus emerging in China is not related to its virulence. J. Virol. 83, 5156–5167.